Hue University Journal of Science: Natural Science
Vol. 132, No. 1D, 15–23, 2023

pISSN 1859-1388
eISSN 2615-9678

# Green synthesis of silver nanomaterials using *Ganoderma Lucidum* extract as reducing agent and stabilizer with ultrasonic assistance and application as an antibacterial agent

**Thu Huong Nguyen[1], Nguyen Vinh Phu[2], Le Thi Hoa[1]*, Thai Hoa Tran[1]**

[1] Department of Chemistry, University of Sciences, Hue University, 77 Nguyen Hue, Hue, Vietnam
[2] Faculty of Basic Sciences, University of Medicine and Pharmacy, Hue University, 06 Ngo Quyen, Hue, Vietnam

* Correspondence to Le Thi Hoa <lethihoa@hueuni.edu.vn>

(*Received: 27 November 2022; Revised: 10 January 2023; Accepted: 10 January 2023*)

**Abstract.** Synthesis of silver nanoparticles (AgNPs) using plant extracts extracted from *Ganoderma lucidum* in the buffer zone of Bach Ma National Park, Vietnam is a simple, convenient, economical, and environmentally friendly method. This study describes the biosynthesis of silver nanoparticles in both cases with and without ultrasonic assistance using *Ganoderma lucidum* extract as a reducing and protective agent. Transmission electron microscopy, scanning electron microscopy, X-ray diffraction, energy-dispersive X-ray spectroscopy, and Fourier transform infrared spectroscopy were used to characterize the as-synthesized AgNPs. Compared to the heating reflux method, the proposed ultrasonic wave assisted heating reflux method produced AgNPs had higher efficiency, smaller and more uniform particle size 6.08 ± 1.80 nm of nm in a short synthesis time period. The antibacterial and antifungal properties of ultrasonically synthesized silver nanomaterials (US-AgNPs) were also investigated. US-AgNPs are important nanomaterials that can find many good applications in practice.

**Keywords:** Silver nanoparticles, *Ganoderma lucidum*, ultrasonic

## 1 Introduction

Today, along with the development of nanotechnology, nano-metallic materials (NPs) have been receiving special attention from domestic and foreign scientists because of their superior properties, such as optical properties, electrical properties, magnetic properties, mechanical properties, and catalytic properties [1]. These properties have opened up many new applications and research opportunities. Precious metal nanomaterials such as Au, Ag, and Pt with particles from 1 to 100 nanometers in size have many unique chemical and optical properties due to surface plasmon resonance (SPR) [2–4]. In particular, silver nanomaterials (AgNPs) have attracted attention because of their potential applications in many different fields, namely biomedical science [5], wastewater treatment [6], agriculture [7], antimicrobial agents and biosensor [8,9], etc. The mechanisms of antibacterial activity of silver nanoparticles (AgNPs) are explained by the fact that AgNPs with small size and large surface area can adhere to the surface of microbial cell membranes, which causes the osmotic and respiratory malfunctions of cells [10]. AgNPs not only interact with the surface of the membranes but can also penetrate into the bacteria [11]. When $Ag^+$ ions interact with the membrane of pathogenic bacteria, they will react with the sulfhydryl group (-SH) of the oxygen-transport enzyme molecules and disable this enzyme, causing the inhibition of cellular respiration, which thereby inactivating the bacteria [12]. These interactions

block DNA replication, thereby killing the bacteria [13].

Currently, silver nanomaterials are synthesized by various physical and chemical methods, such as photochemical reduction [14], chemical reduction [15], using gamma radiation [16], electrochemical [17], hydrothermal [18], microwave [19], ultrasonic waves [20]. However, these methods require modern and expensive equipment, not to mention their harmful effects on the environment and human health. Therefore, the synthetic method, which is called the Green Synthetic Method, uses extracts from plants, bacteria, and fungi [21,22] as both a reducing agent and surface stabilizer without adding other chemicals.

*Ganoderma Lucidum* (*G. lucidum)* is a rare and valuable herb used in traditional medicine. *G. lucidum* contains active ingredients, the most important of which are polysaccharides and triterpenoids [23] with immunomodulatory, free-radicals scavenging, anti-allergic, anti-inflammatory, antiviral, anti-cancer, anti-radiation damage to DNA abilities [24,25].

Many studies have shown that the speed of silver nanomaterial synthesis can be increased using assisted techniques such as microwaves, gamma waves, or ultrasonic waves. In particular, the ultrasonic waves method draws much attention since it requires simple machines and synthesis processes but achieves high efficiency. The ultrasonic wave method is a method that uses ultrasonic waves with wavelengths from 10 cm to $10^{-3}$ cm. This wavelength does not generate enough energy to interact directly with chemical bonds. The ultrasonic wave technique was developed based on the acoustic cavitation phenomenon, which produces air bubbles that form, grow, and collapse in a liquid solution. This collapse generates heat and creates high pressure at the breaking point with extremely high temperature (about 5000), extremely high pressure (about 20 Mpa), and extremely high-temperature rise/fall rate (about $10^{10}$ $K.s^{-1}$) [26]. This process acts as a mediator to receive energy and support the synthesis of silver nanomaterials.

In the scope of this study, silver nanomaterials (AgNPs) were synthesized by the green method using extracts from Lingzhi mushroom (Ganoderma Lucidum), which acts as both a reducing agent and surface stabilizer. Moreover, the advancement of ultrasonic wave assisted synthesis compared to the heating reflux method for prepared AgNPs was successfully demonstrated; furthermore the optical and morphological properties, crystal phase and size distribution of AgNPs were examnined. Then, the synthesized AgNPs material was used to evaluate the antibacterial and antifungal activity.

## 2 Experiment

### 2.1 Materials – Chemicals

**Materials**

The fruiting bodies of *Ganoderma Lucidum* were harvested in the buffer zone of Bach Ma National Park, Nam Dong district, Thua Thien Hue province. They were then dried and ground into powder.

**Chemicals**

Silver nitrate ($AgNO_3 \cdot 5H_2O$, 98%), Amoni hydroxide ($NH_4OH$, 25%), Nitric acid ($HNO_3$, 90%), ethanol 96%(v/v), and Dimethyl sulfoxide (DMSO) 100% were purchased from Xilong Chemical Co., Ltd. All chemicals were used without further purification.

pISSN 1859-1388
eISSN 2615-9678

### 2.2 Preparation of aqueous extract from fruiting bodies of *Ganoderma Lucidum*

Aqueous extraction of *Ganoderma lucidum* was prepared by the previously reported procedure [35]. Briefly, 2.0 g of *Ganoderma Lucidum* powder was added to 200 mL of distilled water. The mixture was refluxed at 85 $^{o}$C for 4 h under stirring conditions. Then, the mixture was centrifuged at 4300 rpm for 20 min to remove the underlying residue and collect the yellowish extract. The yellowish extract was concentrated to 50 mL and then precipitated with ethanol 96% (v/v) at a volume ratio of extract: ethanol of 1: 4. The mixture was kept in the refrigerator for 24 hours, and then centrifuged at 4300 rpm for 20 minutes. The precipitate was washed with acetone and dried at 75 °C for 6 h. The dried aqueous extraction was stored for further experiments.

### 2.3 Biosynthesis of silver nanoparticles

AgNPs were synthesized as per two processes using the heating reflux method (CH-AgNPs) and ultrasonic-assisted heating reflux method (US-AgNPs).

**Synthesis of silver nanomaterials by heating reflux method**

CH-AgNPs were synthesized with optimal synthesis conditions based on published research [27]. The synthesis process is summarized as follows: The dried extract of *G. Lucidum* extract was re-dissolved in water to obtain a *G. Lucidum* extract with a concentration of 1 g/mL. 90 mL of *G. Lucidum* extract was mixed with 10 mL of 1 mM $AgNO_3$ solution. The mixture was adjusted to pH = 9 with $NH_3$ solution (25%). The reduction time was 6 hours, and the reaction temperature was 85°C. The result was the colloidal silver solution, which was then precipitated with ethanol, and centrifuged. The solid fraction was collected and dried at 90°C for 24 hours to obtain CH-AgNPs.

**Synthesis of silver nanomaterials by ultrasonic-assisted heating reflux method**

US-AgNPs were synthesized with an Ultrasound frequency: 42,000 Hz, Heating power: 100 W, Ultrasonic Power: 120 W and were presented as follows: 90 mL of *Ganoderma Lucidum* extract with 1 g/mL concentration was mixed with 10 mL of 1 mM $AgNO_3$ solution, and the mixture was adjusted to pH = 9 with $NH_3$ solution (25%). The mixture was placed in the reaction system, as shown in Figure 1. The reaction was carried out for 1.5 h and the temperature was kept at 60 °C. The resulting colloidal silver solution was then precipitated with ethanol and centrifuged. The solid fraction was collected and dried at 75 °C for 24 h to obtain US-AgNPs.

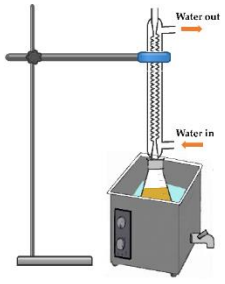


**Fig. 1.** Schematic diagram of the silver nanomaterials synthesis by ultrasonic-assisted heating reflux (US-AgNPs)

### 2.4 Material Characterization Techniques

UV-Vis spectra of AgNPs/GL colloidal solutions were measured on a UV-Vis spectrometer Jasco-V630, Japan. X-ray diffraction was performed on a D8 ADVANCE system (Bruker, Germany). Transmission electron microscopy (TEM) and High-resolution transmission electron microscopy (HR-TEM) images were performed on a JEO, JEM-2100, Japan. The elemental analysis was carried out using energy-dispersive X-ray spectroscopy (EDX, JEOL-6490-JED-200, Japan). Fourier-transform infrared (FTIR) spectrograms were measured on a Nicolet-6700 FTIR spectrometer with a wave-number range of 4000–500 $cm^{-1}$.

### 2.5 Study on antibacterial and antifungal activity of silver nanoparticles

**Dilution of the test sample**

The initial sample was diluted in 2 steps in 100% DMSO and sterilized distilled water into a range of 4-10 concentrations. The highest test concentrations in the test were 256 µg/mL with the extract and 128 µg/mL with the clean substance.

**Test the activities and process the results**

Testing microorganisms were kept at -80 $^0$C. Before the experiment, the testing microorganisms were activated in a culture medium so that the concentration of bacteria reached 5x10$^5$ CFU/ml, and fungal concentration reached 1x10$^3$ CFU/ml. Then, 10 µl of sample solution at different concentrations was placed into a 96-well PCR plate, and 190 µl of the above activated bacterial and fungal solution was added and incubated at 37 $^o$C/16 – 24 hours.

The MIC (Minimum Inhibitor Concentration) value was determined at the well with the lowest reagent concentration that completely inhibited the growth of microorganisms. The IC50 (50% Inhibitor Concentration) value was determined through the percentage value of inhibiting microorganisms from growing and the computer software Raw Data.

$$\%cellularinhibition = \frac{OD_{standard(+)} - OD_{sample}}{OD_{standard(+)} - OD_{standard(-)}}.100\%$$

$$IC_{50} = High_{Conc} - \frac{(High_{Inh\%} - 50).(High_{Conc} - Low_{Conc})}{High_{Inh\%} - Low_{Inh\%}}$$

(In which, High$_{Conc}$/Low$_{Conc}$: reagent at high concentration/low reagent at low concentration; High$_{Inh\%}$/Low$_{Inh\%}$: percentage inhibition at high concentration/ percentage inhibition at low concentration and OD: optical density).

## 3 Results and discussion

### 3.1 Characterization of the obtained materials

In this study, the influence of ultrasonic waves on the synthesis of silver nanomaterials was studied by comparing some characteristics of silver nanomaterials synthesized by two methods: the heating reflux method (CH-AgNPs) and ultrasonic wave method (US-AgNPs).

Before the reaction, the mixture, including the *G. luciudm* aqueous extract and silver nitrate was yellow and after the reaction, the color of the mixture became dark brown color. This alternation of color could be contributed to the confirmation of the formation silver nanoparticles. Moreover, the UV-Vis spectrometer was utilized to study the optical properties of both samples: CH-AgNPs and US-AgNPs.

Figure 2 presents the results of UV-Vis spectra of colloidal silver solution synthesized by two methods: the heating reflux method and the ultrasonic-assisted heating reflux method. From the UV-Vis results, it can be seen that both the two materials samples CH-AgNPs and US-AgNPs have absorption peaks at 425 nm. However, the US-AgNPs sample has higher peak intensity and sharper peak shape than the CH-AgNPs sample.

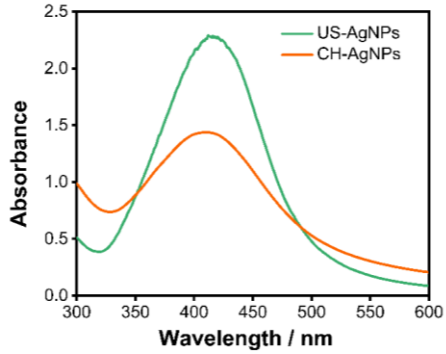


**Fig. 2.** UV-Vis spectra of silver nano colloidal solution synthesized by two methods: the heating reflux method (CH-AgNPs) and ultrasonic-assisted heating reflux method (US-AgNPs)

pISSN 1859-1388
eISSN 2615-9678

From that, it can be predicted that the synthesis of silver nanomaterials by the ultrasonic method has higher efficiency, and the obtained nanoparticles have a more small and uniform size [28].

TEM images reveal the morphology and size distribution of CH-AgNPs and US-AgNPs (Fig. 3). The results show that the morphology of both samples is spherical nanoparticles (Fig. 3a, 3c). Through TEM images and the ImageJ software, Origin 8.5.1, the particle size distributions corresponding CH-AgNPs and US-AgNPs were built (Fig. 3b, 3d). The results of particle size calculation showed that the average particle sizes of CH-AgNPs and US-AgNPs samples were 10.72 ± 2.95 nm and 6.08 ± 1.80 nm, respectively. This shows that samples synthesized with the assistance of ultrasonic waves have smaller particle sizes and more uniform distribution than samples synthesized by the reflux method.

XRD patterns are used to demonstrate the crystal structure of both samples CH-AgNPs and US-AgNPs (Fig. 4). It can be seen that both material samples have four sharp diffraction peaks and completely coincide with the standard spectrum of silver (JCPDS: 03-065-2871) at positions 37.96°, 44.12°, 64.26° and 77.25° for corresponding sides (111), (200), (220) and (311). On the other hand, the crystal size (D) is calculated according to the Sherer equation:

$$D = \frac{K.\lambda}{\beta.\mathrm{Cos}\,\theta}$$

In which: $\beta$ is the width at half peak height; $\beta$ is the diffraction angle (in radians); λ is the wavelength of the X-ray (0.154 nm); K is the Scherrer constant (0.9). XRD diagrams were recorded on a D8-Advanced Bruker instrument (Germany) with Cu anode, recording interval 2θ = 30 - 90°, step angle 0.01°. The results showed that the average crystal size of the US-AgNPs sample (~3.17 nm) was smaller than that of the CH-AgNPs sample (~18.65). The results of the average crystal

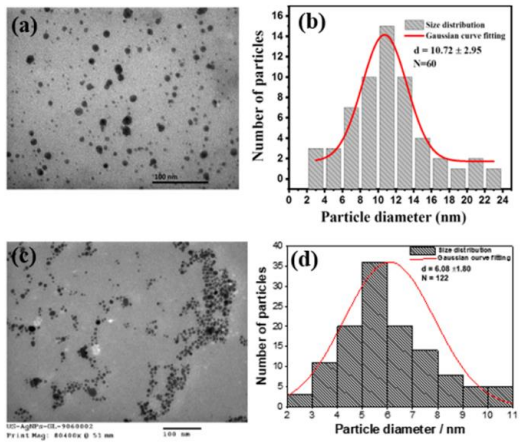


**Fig. 3.** UV-Vis TEM images and the diagrams of the particle size distribution of samples CH-AgNPs (a, b) and US-AgNPs (c, d)

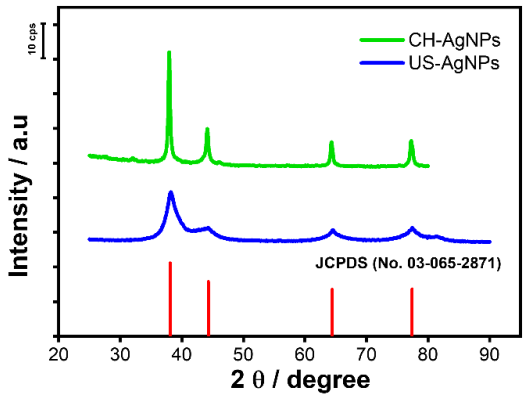


**Fig. 4.** XRD diagram of CH-AgNPs and US-AgNPs material samples

size obtained from XRD spectra had the same pattern as the average particles size gained from TEM images of CH-AgNPs and US-AgNPs. This observation could be explained by comparing the heating mechanism between two methods: the heating reflux method and the ultrasonic-assisted heating reflux method.

The difference in the size of the two samples US-AgNPs and CH-AgNPs is explained based on the effect of ultrasonic waves with their unique properties. Samples of CH-AgNPs were synthesized in a liquid medium and dispersed by mechanical agitation. This solution only increases

the ability to interact between Ag+ ions with organic compounds in the *G. Lucidum* extract.

When ultrasonic waves travel through the tank, waves of compression and expansion are created in the liquid. In the compression wave, the molecules of the reactants are compressed together tightly. Conversely, in the expansion wave, the molecules are pulled apart rapidly [26]. The expansion is so dramatic that the molecules are ripped apart, creating microscopic bubbles. The continuous compression and expansion of microscopic bubbles in the solution create vortices, help the reaction mixture to be diffused strongly, and keep the reaction mixture homogeneous [29]. The collapse of the microscopic bubbles generates a tremendous amount of heat and pressure [30], which causes small-scale reaction centres throughout the solution and increases the rate of the reduction reaction of $Ag^{+}$ to $Ag^{0}$. In addition, ultrasonic waves are mechanical waves, so they have a mechanical effect on the reaction mixture, acting as a surface protection agent and preventing silver nanoparticles from clumping together. Therefore, the obtained US-AgNPs material sample has smaller and more uniform silver nanoparticles compared to the CH-AgNPs material sample.

The HR-TEM imaging technique was used to study the morphological and surface characteristics of silver nanoparticles in the US-AgNPs sample. The HR-TEM image of the US-AgNPs material presented in Fig. 5 shows that the silver nanoparticles are spherical, located separately, and have parallel lines, indicating that these are crystals and indicating that these are crystals and the interplanar (111) distance of 0.22 nm.

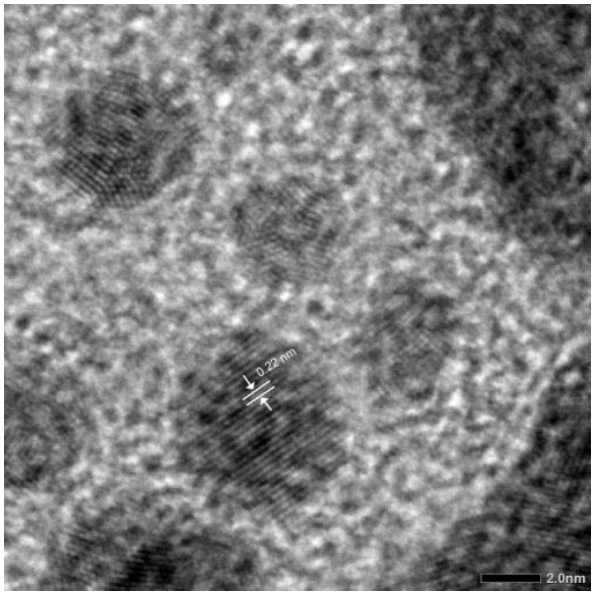


**Fig. 5.** HR-TEM image of US-AgNPs sample

FT-IR spectroscopy was performed to demonstrate functional groups capping on the surface of AgNPs. Figure 6 shows the FT-IR spectra of *G. lucidum* extract, US-AgNPs. In the spectrum of *G. lucidum*, the absorption peak observed at 3408 $cm^{-1}$ was attributed to the stretching vibration of hydroxyl groups [31,32]. In addition, it has peaked at 2914 and 1614 cm−1, corresponding to methylene and carbonyl groups, respectively, and the peak appearing at ~2918 cm−1 was attributed to

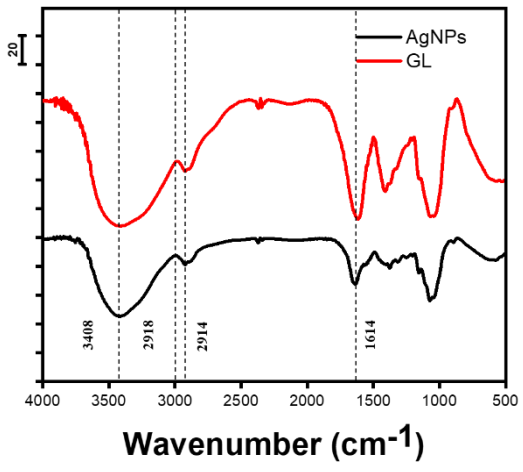


**Fig. 6.** FT-IR spectra of G. lucidum extract and US-AgNPs

pISSN 1859-1388
eISSN 2615-9678

the stretching of the C-N group [31]. The spectra of US-AgNPs are similar to the spectra of *G. lucidum*, leading to the that there were certain functional groups on the surface of silver nanoparticles.

The elemental composition of US-AgNPs was examined by using the EDX technique; furthermore, the EDX elemental mapping was observed in Fig. 7. The component elements, including C, O, and Ag accounted for 9.59%: 5.71%: 84.70%, respectively, by mass (Table 1). The distribution of elements C, O, and Ag in the AgNPs material sample is presented in Figure 7. b, c, and d. It can be seen that elemental silver is evenly distributed throughout the US-AgNPs sample.

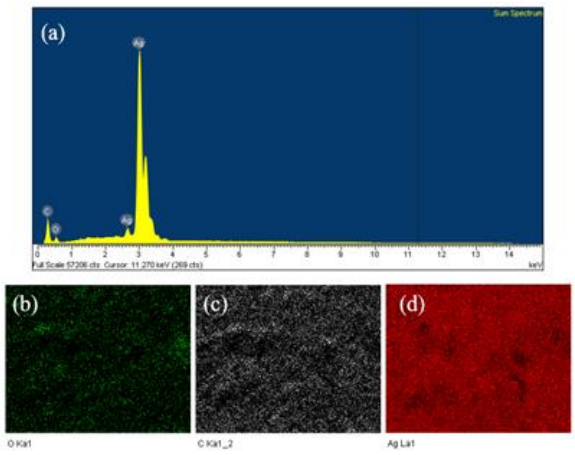


**Fig. 7.** EDX spectrum and SEM-Mapping images of the elemental distribution map of US-AgNPs material samples

**Table 1.** The elemental composition of MW-AuNPs was analyzed using EDX

| Element | Weight (%) | Atom (%) |
|---|---|---|
| C | 9.59 | 41.14 |
| O | 5.71 | 18.40 |
| Ag | 84.70 | 40.47 |

From the above results, it can be seen that the effect of ultrasonic waves makes the reaction time shorter, the synthesis efficiency high, and the material particle and crystal size smaller. The samples of silver nanoparticles synthesized with the assistance of ultrasonic waves are further used to conduct test on the antibacterial and antifungal properties.

### 3.2 Antibacterial and anti-fungal ability

The inhibitory effect on tested microorganisms is shown in Table 2. The results showed that silver nanomaterials have inhibitory ability against seven strains of bacteria and fungi, namely Gram (+): *S. aureus*, *B. subtilis*, *L. fermentum*; Gram (-): *S. enterica*, *E. coli*, *P.aeruginosa* and *C.albicans* fungus at concentrations from 1 μg/mL to 256 μg/mL. In general, samples of US-AgNPs have high antibacterial ability against Gram (+) and Gram (-) strains with $IC_{50}$ value < 5.0 (μg/mL) (except *B.subtilis* which is 34.7 μg/mL) and the MIC ranged from 4 to 16 (μg/mL). However, the resistance to *C.albican* fungus is not good with $IC_{50}$ and MIC values of 145.84 and >256 μg/mL, respectively.

In general, the ability to inhibit all strains of Gram-positive and Gram-negative bacteria of silver nanomaterials is very strong with $IC_{50}$ values < 5.0 (μg/mL) (except *B.subtilis*, which is 34.7 μg/mL) and MICs in the range of 4-16 (μg/mL). This proves that silver nanomaterials have potential in their application as valuable biosafety antibiotics.

**Table 2.** Inhibitory effect on seven strains of microorganisms and fungi

| No | Sample | Value (μg/mL) | % Inhibition of tested microbial and fungal strains | | | | | | |
|---|---|---|---|---|---|---|---|---|---|
| | | | Gram (+) | | | Gram (-) | | | Fungi |
| | | | *S.aureus* | *B. subtilis* | *L.fermentum* | *S.enterica* | *E.coli* | *P.aeruginosa* | *C.albican* |
| US-AgNPS | | 256 | 97 | 95 | 99 | 99 | 99 | 99 | 67.5 |
| | | 64 | 92 | 65 | 99 | 99 | 99 | 99 | 37 |
| | | 16 | 92 | 40.5 | 97 | 98.5 | 94 | 98 | 24 |
| | | 4 | 89.5 | 21 | 72 | 54 | 93 | 97 | 21 |

| No | Sample | Value (μg/mL) | % Inhibition of tested microbial and fungal strains | | | | | | |
|---|---|---|---|---|---|---|---|---|---|
| | | | Gram (+) | | | Gram (-) | | | Fungi |
| | | | *S.aureus* | *B. subtilis* | *L.fermentum* | *S.enterica* | *E.coli* | *P.aeruginosa* | *C.albican* |
| | | 1 | 45.5 | 3 | 21.5 | 4 | 46.5 | 45.5 | 6 |
| | | $IC_{50}$ | 1.30±0.05 | 34.7±0.70 | 2.70±0.11 | 3.76±0.14 | 1.22±0.04 | 1.26±0.03 | 145.84±0.62 |
| | | MIC | 4 | 256 | 16 | 16 | 4 | 4 | >256 |

## 4 Conclusion

In this study, we presented a process to synthesize silver nanomaterials by the "green method" by both the heating reflux method and the ultrasonic wave assisted heating reflux method using extracts from *Ganoderma Lucidum* as a reducing and protective agent. The results show that the synthesis of silver nanomaterials by ultrasonic-assisted heating reflux method has higher efficiency, a shorter reaction time, and a smaller and more uniform size of obtained nanoparticles compared to the heating reflux method.

The synthesized silver nanoparticles have effective antibacterial and antifungal properties, opening up many potential applications in medicine and many other fields.

## Acknowledgement

This work was partially supported by Hue University under the Core Research Program, Grant No. NCM.DHH.2022.04.

## References

1. Yokoyama S, Takahashi H, Itoh T, Motomiya K, Tohji K. Synthesis of metallic Cu nanoparticles by controlling Cu complexes in aqueous solution. Adv Powder Technol. 2014;25(3):999-1006.
2. Millstone JE, Hurst SJ, Métraux GS, Cutler JI, Mirkin CA. Colloidal gold and silver triangular nanoprisms. Small. 2009;5(6):646-64.
3. Lee SH, Rho WY, Park SJ, Kim J, Kwon OS, Jun BH. Multifunctional self-assembled monolayers via microcontact printing and degas-driven flow guided patterning. Sci Rep. 2018;8(1):1-8.
4. Lee SH, Sung JH, Park TH. Nanomaterial-based biosensor as an emerging tool for biomedical applications. Ann Biomed Eng. 2012;40(6):1384-97.
5. Chaloupka K, Malam Y, Seifalian AM. Nanosilver as a new generation of nanoproduct in biomedical applications. Trends Biotechnol. 2010;28(11):580-8.
6. Dankovich TA, Gray DG. Bactericidal paper impregnated with silver nanoparticles for point-of-use water treatment. Environ Sci Technol. 2011;45(5):1992-8.
7. Holt KB, Bard AJ. Interaction of silver (I) ions with the respiratory chain of Escherichia coli: an electrochemical and scanning electrochemical microscopy study of the antimicrobial mechanism of micromolar Ag+. Biochemistry. 2005;44(39):13214-23.
8. Vaseem M, Lee KM, Hong AR, Hahn YB. Inkjet printed fractal-connected electrodes with silver nanoparticle ink. ACS Appl Mater Interfaces. 2012;4(6):3300-7.
9. Xu W, Jin W, Lin L, Zhang C, Li Z, Li Y, et al. Green synthesis of xanthan conformation-based silver nanoparticles: antibacterial and catalytic application. Carbohydr Polym. 2014;101:961-7.
10. Kvítek L, Panáček A, Soukupova J, Kolář M, Večeřová R, Prucek R, et al. Effect of surfactants and polymers on stability and antibacterial activity of silver nanoparticles (NPs). J Phys Chem C. 2008;112(15):5825-34.
11. Morones JR, Elechiguerra JL, Camacho A, Holt K, Kouri JB, Ramírez JT, et al. The bactericidal effect of silver nanoparticles. Nanotechnology. 2005;16(10):2346-53.
12. Gupta A, Maynes M, Silver S. Effects of halides on plasmid-mediated silver resistance in Escherichia coli. Appl Environ Microbiol. 1998;64(12):5042-5.
13. Melaiye A, Sun Z, Hindi K, Milsted A, Ely D, Reneker DH, et al. Silver (I)− imidazole cyclophane

pISSN 1859-1388
eISSN 2615-9678

gem-diol complexes encapsulated by electrospun tecophilic nanofibers: Formation of nanosilver particles and antimicrobial activity. J Am Chem Soc. 2005;127(7):2285-91.

14. Khan Z, Al-Thabaiti SA, Obaid AY, Al-Youbi AO. Preparation and characterization of silver nanoparticles by chemical reduction method. Colloids Surfaces B Biointerfaces. 2011;82(2):513-7.
15. Chen P, Song L, Liu Y, Fang Y e. Synthesis of silver nanoparticles by γ-ray irradiation in acetic water solution containing chitosan. Radiat Phys Chem. 2007;76(7):1165–8. https://doi.org/10.1016/j.radphyschem.2006.11.012.
16. 16.Zhang W, Qiao X, Chen J. Synthesis and characterization of silver nanoparticles in AOT microemulsion system. Chem Phys. 2006;330(3):495-500.
17. Abid JP, Wark AW, Brevet PF, Girault HH. Preparation of silver nanoparticles in solution from a silver salt by laser irradiation. Chem Commun. 2002;(7):792-3.
18. Yang J, Pan J. Hydrothermal synthesis of silver nanoparticles by sodium alginate and their applications in surface-enhanced Raman scattering and catalysis. Acta Mater. 2012;60(12):4753-8.
19. Nas MS, Calimli MH. Recent Development of Nanoparticle by Green-Conventional Methods and Applications for Corrosion and Fuel Cells. Curr Nanosci. 2021;17(4):525-39.
20. Alarcon EI, Udekwu K, Skog M, Pacioni NL, Stamplecoskie KG, González-Béjar M, et al. The biocompatibility and antibacterial properties of collagen-stabilized, photochemically prepared silver nanoparticles. Biomaterials. 2012;33(19):4947-56.
21. Venkatesan J, Kim SK, Shim MS. Antimicrobial, antioxidant, and anticancer activities of biosynthesized silver nanoparticles using marine algae Ecklonia cava. Nanomaterials. 2016;6(12):235.
22. Paulkumar K, Gnanajobitha G, Vanaja M, Rajeshkumar S, Malarkodi C, Pandian K, et al. Piper nigrum leaf and stem assisted green synthesis of silver nanoparticles and evaluation of its antibacterial activity against agricultural plant pathogens. Sci World J. 2014;2014.
23. Boh B, Berovic M, Zhang J, Zhi-Bin L. Ganoderma lucidum and its pharmaceutically active compounds. Biotechnol Annu Rev. 2007;13:265-301.
24. Ma HT, Hsieh JF, Chen ST. Anti-diabetic effects of Ganoderma lucidum. Phytochemistry. 2015;114:109-13.
25. Pan K, Jiang Q, Liu G, Miao X, Zhong D. Optimization extraction of Ganoderma lucidum polysaccharides and its immunity and antioxidant activities. Int J Biol Macromol. 2013;55:301-6.
26. Dang F, Enomoto N, Hojo J, Enpuku K. Sonochemical coating of magnetite nanoparticles with silica. Ultrason Sonochem. 2010;17(1):193-9.
27. Nguyen VP, Le Trung H, Nguyen TH, Hoang D, Tran TH. Synthesis of Biogenic Silver Nanoparticles with Eco-Friendly Processes Using Ganoderma lucidum Extract and Evaluation of Their Theranostic Applications. Journal of Nanomaterials. 2021;2021:6135920.
28. Seifipour R, Nozari M, Pishkar L. Green synthesis of silver nanoparticles using Tragopogon collinus leaf extract and study of their antibacterial effects. J Inorg Organomet Polym Mater. 2020;1-11.
29. Wani IA, Ganguly A, Ahmed J, Ahmad T. Silver nanoparticles: ultrasonic wave assisted synthesis, optical characterization and surface area studies. Mater Lett. 2011;65(3):520-2.
30. Xu H, Zeiger BW, Suslick KS. Sonochemical synthesis of nanomaterials. Chem Soc Rev. 2013;42(7):2555-67.
31. Wang J, Zhang L. Structure and chain conformation of five water-soluble derivatives of a β-D-glucan isolated from Ganoderma lucidum. Carbohydr Res. 2009;344(1):105-12.
32. Ibrahim M, Alaam M, El-Haes H, Jalbout AF, De Leon A. Analysis of the structure and vibrational spectra of glucose and fructose. Eclet Quim. 2006;31(3):15-21.